Supplementary data to:

Reduction of obesity-associated white adipose tissue inflammation by rosiglitazone is associated with reduced non-alcoholic fatty liver disease in LDLr-deficient mice

Petra Mulder[1,2*], Martine C. Morrison[1], Lars Verschuren[3], Wen Liang[1], J. Hajo van Bockel[2], Teake Kooistra[1], Peter Y. Wielinga[1], Robert Kleemann[1,2]

[1] Department of Metabolic Health Research, Netherlands Organization for Applied Scientific Research (TNO), Zernikedreef 9, 2333 CK Leiden, The Netherlands

[2] Department of Vascular Surgery, Leiden University Medical Center, PO Box 9600, 2300 RC Leiden, The Netherlands

[3] Department of Microbiology and Systems Biology, Netherlands Organization for Applied Scientific Research (TNO), 3704 HE, Zeist, The Netherlands

***** Corresponding author, email: petra.mulder@tno.nl

Supplement 1: Effect of rosiglitazone intervention on inflammatory CCR2-positive and CD11c-positive immune cells in adipose tissue

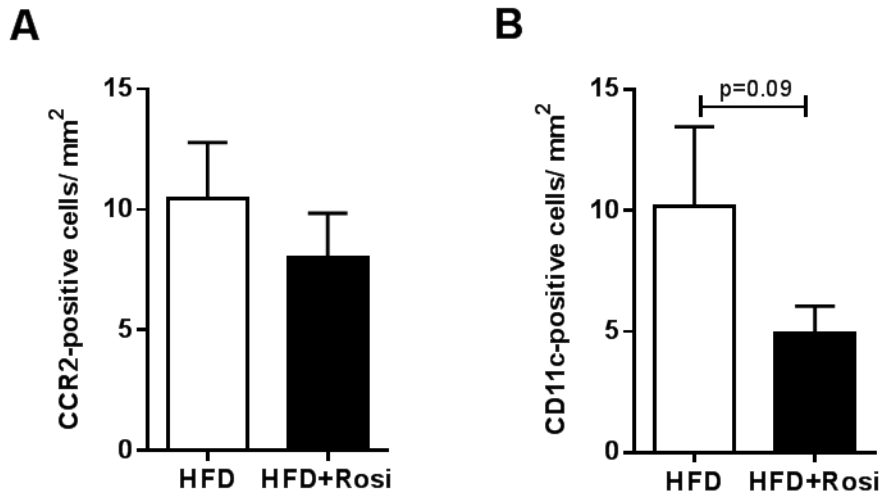

Supplementary figure 1. To investigate whether rosiglitazone intervention modulates adipose tissue immune cell activation, we have performed immunohistochemical stainings using primary antibodies against CCR2 and CD11c on adipose tissue cross-sections of mice fed a high-fat diet (HFD) or a HFD supplemented with rosiglitazone (HFD+Rosi). We found less immunoreactivity against CCR2 (**Supplementary figure 1A**) and CD11c (**Supplementary figure 1B**) in mice treated with rosiglitazone, which is consistent with the gene expression data. Values are expressed as mean±SEM and expressed as positively stained cells per mm^2 adipose tissue (n=4/group).

Supplement 1 *continued*

C

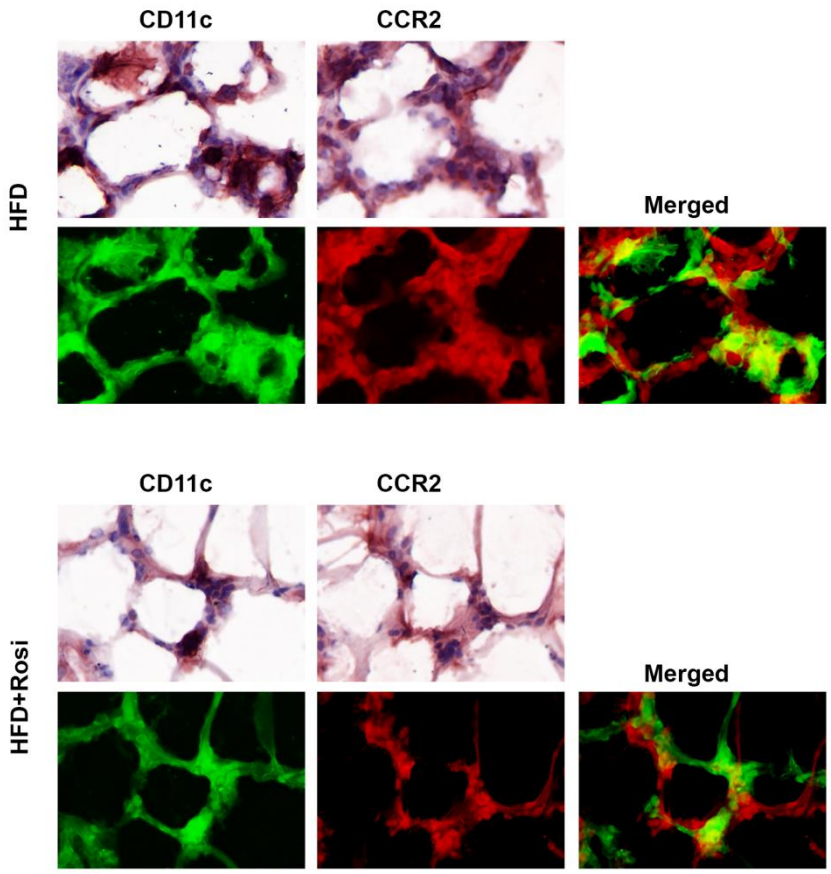

Supplementary figure 1C shows representative pictures of a crown-like structure (CLS) in adipose tissue of HFD-fed mice and HFD+Rosi mice, which stained positively for CCR2 and CD11c (dark brown staining, upper panels). In order to merge the coloring of the two different immunostainings in a CLS, the bright field images were converted to 8-bit immunofluorescent images (lower panels). The immunoreactivity against CD11c and CCR2 is shown in green and red, respectively. The merged images demonstrate that CLS in the HFD group and the HFD+Rosi group contain CCR2+ and CD11c+ cells and some of these cells express both markers (overlap is indicated by yellow). (Microphotographs: magnification x200).

Supplement 2: Microarray analysis of the effects of rosiglitazone intervention in WAT

Gene set enrichment showed that rosiglitazone intervention significantly affected several biological canonical pathways related to inflammatory oxidative stress in WAT. These pathways can be grouped in three main clusters shown below and specified in **Supplementary Figure 2A-1.**

1) Oxidative phosphorylation/ Mitochondrial dysfunction
2) Oxidative stress response/peroxisomal response
3) Acute phase response/ fibrosis

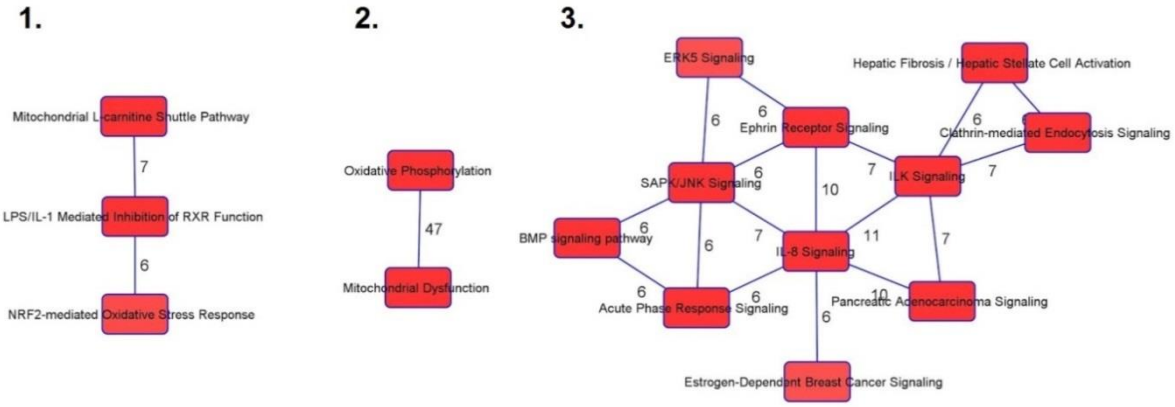

Supplementary Figure 2A-1. Clustering of canonical pathways that are influenced by rosiglitazone intervention. This graph shows three clusters, each of which consisting of canonical pathways. Lines between two pathways indicate that these pathways share genes (the number of overlapping genes is mentioned). The significance of the effect of rosiglitazone on individual pathways is provided in the figure below.

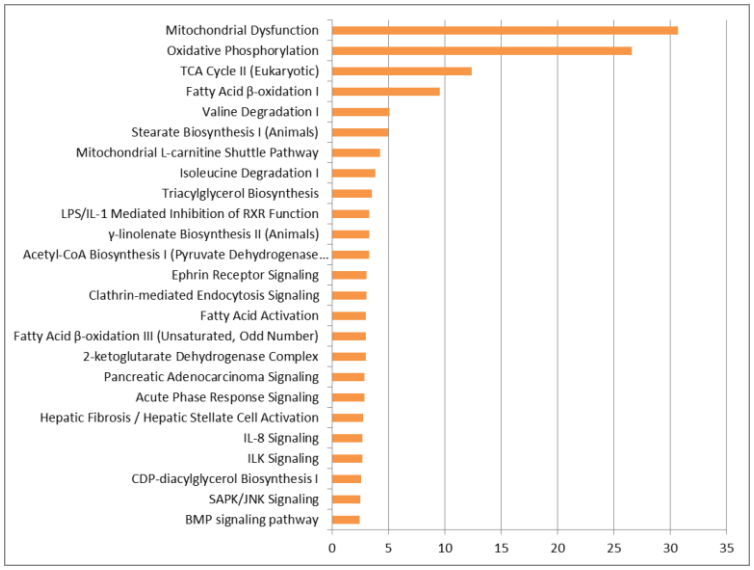

Supplementary Figure 2A-2. Canonical pathways influenced by rosiglitazone. The bars in the figure indicate significance of the different pathways. Significance is expressed as -log p-values.

As an example for the anti-inflammatory effect of rosiglitazone in WAT, the individual genes of the canonical pathway 'Acute phase response signaling' are listed below (**Supplementary Table 2A**). Among the genes that were reduced by rosiglitazone were complement factors, kinases and acute phase reactants such as haptoglobin, serum amyloid A3 and von Willebrand factor.

Supplementary Table 2A.

geneSymbol	geneName	Log Ratio	*p*-value
AGT	angiotensinogen (serpin peptidase inhibitor, clade A, member 8)	-2,45	2,50E-08
C2	complement component 2	-1,345	2,69E-07
C4A/C4B	complement component 4B (Chido blood group)	-1,471	7,47E-09
CFB	complement factor B	-1,856	2,67E-08
HP	haptoglobin	-3,09	4,83E-14
HRAS	Harvey rat sarcoma viral oncogene homolog	0,661	3,62E-03
KRAS	Kirsten rat sarcoma viral oncogene homolog	0,677	7,21E-06
LBP	lipopolysaccharide binding protein	-2,18	8,91E-08
MAPK12	mitogen-activated protein kinase 12	-0,527	5,78E-03
MTOR	mechanistic target of rapamycin (serine/threonine kinase)	0,466	1,13E-03
OSMR	oncostatin M receptor	-0,7	4,47E-05
RBP7	retinol binding protein 7, cellular	2,14	8,13E-09
RELA	v-rel avian reticuloendotheliosis viral oncogene homolog A	-0,417	4,28E-03
RIPK1	receptor (TNFRSF)-interacting serine-threonine kinase 1	-0,276	8,71E-03
RRAS	related RAS viral (r-ras) oncogene homolog	-0,649	1,55E-03
Saa3	serum amyloid A 3	-2,635	3,81E-05
SERPINA3	serpin peptidase inhibitor, clade A (alpha-1 antiproteinase, antitrypsin), member 3	-2,923	3,69E-31
SERPING1	serpin peptidase inhibitor, clade G (C1 inhibitor), member 1	-0,659	7,50E-04
SOCS5	suppressor of cytokine signaling 5	0,455	3,79E-03
TAB1	TGF-beta activated kinase 1/MAP3K7 binding protein 1	-0,415	8,28E-03
TF	transferrin	-0,933	1,07E-04
VWF	von Willebrand factor	-1,115	4,49E-04

Supplement 2 *continued*

Supplementary table 2B. Differentially expressed PPARγ regulated genes in epididymal white adipose tissue affected by rosiglitazone intervention in LDLr-/- mice. Transcriptional network analysis demonstrated a significant transcriptional activation of PPARγ (high and positive Z-score of 4.1, *p*=5.92e-24). Rosiglitazone significantly affected the transcription of 71 PPARγ regulated genes in WAT as listed below. False discovery rate of 5% (FDR<0.05) was used.

eWAT	**HFD+Rosi compared with HFD**	
Genes in dataset	**Prediction (based on expression direction)**	**Log Ratio**
UCP1	Activated	3.351
TSC22D3	Activated	-0.799
SORBS1	Activated	0.795
SOD1	Activated	0.542
SLC27A1	Activated	1.810
SLC25A20	Activated	1.399
SLC25A1	Activated	0.991
PPARGC1B	Activated	0.935
PMM1	Activated	1.260
PLIN5	Activated	2.068
PDK4	Activated	3.228
MGLL	Activated	1.015
ME1	Activated	1.048
MDH1	Activated	0.863
HP	Activated	-3.090
HADHB	Activated	1.175
GPD1	Activated	2.167
GDF15	Activated	1.279
FABP5	Activated	1.361
FABP3	Activated	2.700
ESRRA	Activated	0.490
EPHX1	Activated	-0.546
EHHADH	Activated	2.244
DLAT	Activated	1.142
CYP4B1	Activated	1.784
CS	Activated	0.911
CRAT	Activated	1.018
CPT2	Activated	1.249
CPT1B	Activated	3.491
CIDEA	Activated	3.514
CAT	Activated	1.016
ATP5O	Activated	1.204
AQP7	Activated	1.205
APP	Activated	-0.551

Supplementary table 2B continued

eWAT	**HFD+Rosi compared with HFD**	
Genes in dataset	**Prediction (based on expression direction)**	**Log Ratio**
ADIG	Activated	0.902
ACTA2	Activated	-1.767
ACSL1	Activated	1.200
ACOX1	Activated	1.222
ACADS	Activated	1.566
ACADM	Activated	1.035
ACAA2	Activated	1.116
Acaa1b	Activated	1.927
VEGFA	Inhibited	-1.435
PRODH	Inhibited	-1.418
PPIC	Inhibited	-0.959
PPARGC1A	Inhibited	0.934
MLYCD	Inhibited	1.078
LAMB3	Inhibited	-1.329
GATA2	Inhibited	-0.889
ELOVL6	Inhibited	-1.391
CFD	Inhibited	-1.274
CCND1	Inhibited	-0.791
APOE	Inhibited	-0.737
ACSL5	Inhibited	-0.576
Abcb1b	Inhibited	-0.826
ACADL	Affected	1.571
ACOT8	Affected	0.575
AGT	Affected	-2.450
CDK2	Affected	-0.597
FBP2	Affected	1.359
HR	Affected	-1.589
HSD3B7	Affected	-0.842
IGFBP3	Affected	-1.141
IGFBP5	Affected	-1.650
IGFBP7	Affected	-0.404
PDHB	Affected	0.850
S100A8	Affected	-2.150
SCNN1G	Affected	1.209
SCP2	Affected	1.216
UGT1A9 (includes others)	Affected	-1.200
VLDLR	Affected	0.723

Supplement 3: Rosiglitazone intervention does not activate PPAR-regulated genes in livers of LDLr-/- mice

Original transcriptomics data: http://www.ebi.ac.uk/arrayexpress/experiments/E-MTAB-1063/

Supplement 3A: Table listing 36 genes that are differentially expressed by rosiglitazone in liver.

probeID	geneSymbol	geneName	Log Ratio	Adjusted p-value
ILMN_2925947	ABAT	4-aminobutyrate aminotransferase	0,505	4,05E-02
ILMN_2629112	ACER2	alkaline ceramidase 2	0,68	5,03E-03
ILMN_2965414	ANKRD22	ankyrin repeat domain 22	0,94	4,83E-06
ILMN_2834123	APOA4	apolipoprotein A-IV	-2,376	4,48E-03
ILMN_2641301	APOA5	apolipoprotein A-V	-0,823	9,36E-03
ILMN_2732601	ARSG	arylsulfatase G	-0,745	9,36E-03
ILMN_2776603	Ccl9	chemokine (C-C motif) ligand 9	0,621	1,75E-02
ILMN_2835423	CFD	complement factor D (adipsin)	4,666	1,33E-06
ILMN_2609813	CHI3L1	chitinase 3-like 1 (cartilage glycoprotein-39)	1,455	1,88E-02
ILMN_1215446	CIDEA	cell death-inducing DFFA-like effector a	3,387	1,99E-03
ILMN_2827217	CLSTN3	calsyntenin 3	1,349	1,03E-02
ILMN_2806996	CREB3L3	cAMP responsive element binding protein 3-like 3	-0,52	3,19E-03
ILMN_2960325	CTSE	cathepsin E	0,926	3,24E-02
ILMN_2664224	EPHX1	epoxide hydrolase 1, microsomal (xenobiotic)	-0,657	4,60E-02
ILMN_2710698	FGF21	fibroblast growth factor 21	-1,51	2,59E-02
ILMN_2605941	GNPAT	glyceronephosphate O-acyltransferase	0,389	1,67E-02
ILMN_3007956	GZF1	GDNF-inducible zinc finger protein 1	0,398	4,72E-02
ILMN_2795520	HLA-A	major histocompatibility complex, class I, A	-0,523	2,71E-02
ILMN_2662160	IMPA2	inositol(myo)-1(or 4)-monophosphatase 2	-0,779	4,48E-03
ILMN_1229605	INHBE	inhibin, beta E	-0,918	3,24E-02
ILMN_2692723	LPL	lipoprotein lipase	1,261	2,51E-04
ILMN_1225764	MFSD2A	major facilitator superfamily domain containing 2A	-1,977	2,58E-02
ILMN_2813830	NT5E	5'-nucleotidase, ecto (CD73)	0,992	3,69E-02
ILMN_2680628	Pbld2	phenazine biosynthesis-like protein domain containing 2	-0,442	3,20E-02
ILMN_2924754	PDZK1	PDZ domain containing 1	-0,315	7,40E-03
ILMN_1249694	PGM3	phosphoglucomutase 3	-0,536	3,20E-02
ILMN_2739760	PRELP	proline/arginine-rich end leucine-rich repeat protein	-0,429	1,88E-02
ILMN_1254902	RDH16	retinol dehydrogenase 16 (all-trans)	1,318	1,33E-06
ILMN_1240471	RETSAT	retinol saturase (all-trans-retinol 13,14-reductase)	-0,719	1,88E-02
ILMN_2825446	SDCBP2	syndecan binding protein (syntenin) 2	1,575	3,19E-03
ILMN_2684145	SDCBP2	syndecan binding protein (syntenin) 2	0,999	7,40E-03
ILMN_2826264	SERINC2	serine incorporator 2	-0,72	1,88E-02
ILMN_1231573	SERPINB1	serpin peptidase inhibitor, clade B (ovalbumin), member 1	1,994	4,83E-06
ILMN_1256644	SLC6A12	solute carrier family 6 (neurotransmitter transporter), member 12	0,482	2,58E-02
ILMN_2695199	ST3GAL6	ST3 beta-galactoside alpha-2,3-sialyltransferase 6	0,826	5,02E-05
ILMN_2757599	TSPAN31	tetraspanin 31	-0,415	5,62E-04
ILMN_1236758	WFDC2	WAP four-disulfide core domain 2	-2,028	1,18E-03

Supplement 3B: Specific analysis of PPARγ-regulated genes in liver

Only 4 out of the 36 differentially expressed genes in the liver can potentially be regulated by PPARγ. These 4 genes are listed below. However, also other transcriptional regulators control the expression of these genes and a composite analysis of all gene expression changes (see upstream transcriptional regulator analysis below) shows that PPARγ is not activated.

Liver	**HFD+Rosi compared with HFD control**	
Genes in dataset	**Prediction (based on expression direction)**	**Log Ratio**
CFD	Activated	4.666
CIDEA	Activated	3.387
LPL	Activated	1.276
EPHX1	Activated	-0.657

Supplement 3C: Upstream transcriptional regulator analysis for PPARγ, PPARα and PPARδ in liver

Transcriptional network analysis of differentially expressed genes in liver demonstrated that there is no significant transcriptional activation of upstream regulators PPARγ, PPARα or PPARδ by rosiglitazone. False discovery rate of 5% (FDR<0.05) was used.

As reference for the validity of the method and for PPARα activation, we have used livers from LDLr-/- mice treated with fenofibrate (0.05% w/w), a pharmacological ligand of PPARα. Diets and duration of intervention were the same as for rosiglitazone. Fenofibrate significantly activates PPARα activity (Z-score: 7.9, p =4.5e-55) based on gene expression changes induced by fenofibrate. Consistent with this, a significant activation of several key processes of lipid metabolism in liver was observed with fenofibrate (see **Supplementary Table 3C**). These processes were not affected with rosiglitazone treatment. In line with this, hepatic concentrations of β-hydroxybutyrate (beta-oxidation product) were increased with fenofibrate treatment, but not with rosiglitazone (**Supplementary Figure 3C**), further supporting absence of PPARα activation by rosiglitazone.

Supplementary Table 3C

Top bio functions in lipid metabolism	**Predicted Activation State**	**Log ratio**	***p*-value**
transport of long chain fatty acid	Increased	2,902	1,91E-09
oxidation of fatty acid	Increased	2,782	1,04E-17
uptake of long chain fatty acid	Increased	2,634	1,20E-03
storage of lipid	Increased	2,58	3,39E-06

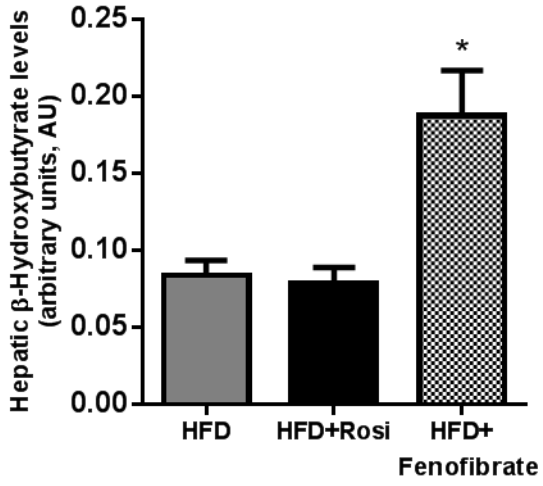

Supplementary figure 3C Using liver tissue homogenates and GC-MS technology, we examined whether rosiglitazone would affect hepatic β-hydroxybutyrate levels (a marker of hepatic fatty acid oxidation) relative to HFD mice. As a positive control for activation of PPARα, livers of fenofibrate-treated LDLr-/- mice were used. The levels of hepatic β-hydroxybutyrate were not increased by rosiglitazone, but were significantly increased by fenofibrate. These data further support absence of PPARα activation by rosiglitazone. Values are expressed as mean ± SEM and expressed as arbitrary units (AU) relative to internal standard. *$p<0.05$ vs. HFD, HFD+Rosi.

Supplement 4: Effect of rosiglitazone on myeloperoxidase (MPO)-positive cells (neutrophils) in liver

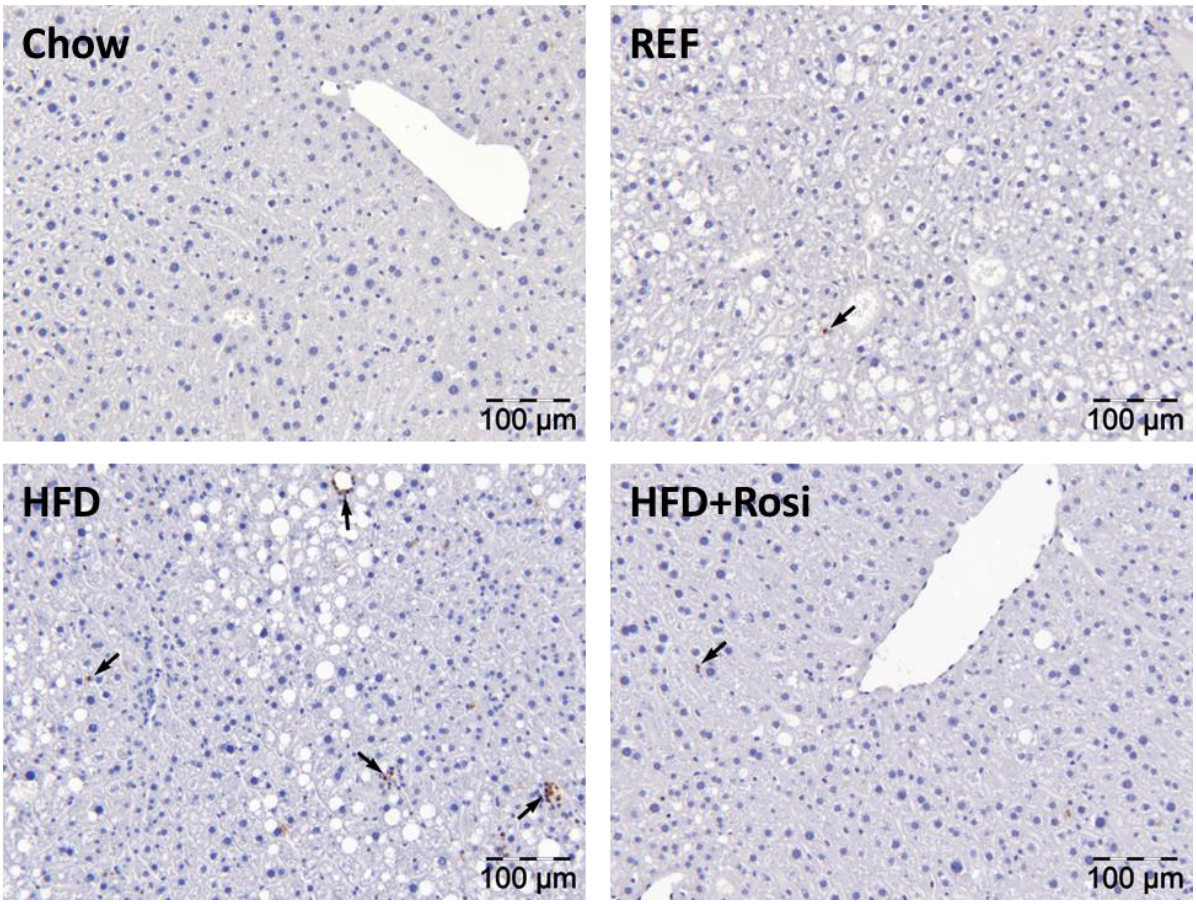

Representative pictures of MPO immunohistochemical stained liver sections of mice after a chow diet, 9 or 16 weeks high-fat diet (REF and HFD, respectively) or rosiglitazone intervention (HFD+Rosi). Infiltration of neutrophils into the liver was observed after 16 weeks of HFD (both single cells and cell aggregates). Only a few MPO-positive cells were observed in HFD+Rosi, which resembled the condition prior to intervention (REF). (magnification x100).

Supplement 5: Effect of rosiglitazone on adipokine plasma concentrations of leptin, TNFα and adiponectin

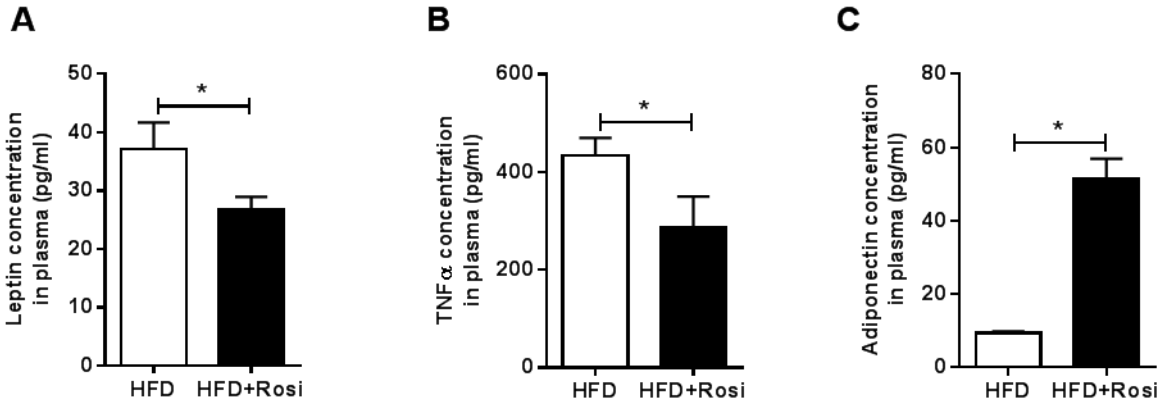

Plasma concentrations of (A) leptin, (B) TNFα, and (C) adiponectin of mice fed either a high-fat diet (HFD) or a HFD supplemented with rosiglitazone (HFD+Rosi). Rosiglitazone intervention reduced levels of pro-inflammatory adipokines leptin and TNFα. By contrast, rosiglitazone increased levels of anti-inflammatory adipokine adiponectin. Values are expressed as mean±SEM and expressed as plasma concentrations in pg/ml. *$p<0.05$.